Available online at www.sciencedirect.com
SCIENCE DIRECT
International Journal of Pharmaceutics 308 (2006) 69–83
INTERNATIONAL JOURNAL OF PHARMACEUTICS
www.elsevier.com/locate/ijpharm

Use of compressed gas precipitation to enhance the dissolution behavior of a poorly water-soluble drug: Generation of drug microparticles and drug–polymer solid dispersions

Gerhard Muhrer [a], Ulrich Meier [a], Francesco Fusaro [b], Siria Albano [b], Marco Mazzotti [b,*]

[a] *Novartis Pharma AG, Chemical & Analytical Development, CH-4002 Basel, Switzerland*
[b] *ETH Swiss Federal Institute of Technology Zurich, Institute of Process Engineering, Sonneggstrasse 3, CH-8092 Zurich, Switzerland*

Received 27 June 2005; received in revised form 18 October 2005; accepted 20 October 2005
Available online 1 December 2005

Abstract

The classical anticonvulsant drug phenytoin (5,5-diphenyl hydantoin, $C_{15}H_{12}N_2O_2$) has been used as a model compound to investigate the possibility of enhancing the dissolution rate of poorly water-soluble drugs using dense gas antisolvent techniques. In a first step, microcrystals of neat phenytoin have been generated using the gas antisolvent (GAS) and precipitation with compressed antisolvent (PCA) processes, thereby assessing process performances and elucidating similarities and differences between the two techniques. In a second step, the PCA process has been used to generate solid dispersions of phenytoin in the hydrophilic polymer poly(vinyl-pyrrolidone)-K30 (PVP). In vitro dissolution results reveal a substantially better performance of the PCA-processed co-formulations compared to unprocessed phenytoin and to GAS- and PCA-precipitates of neat drug crystals. A comparison of the product quality of phenytoin–PVP co-formulations with solid dispersions obtained by spray drying convincingly underlines the potential of dense gas antisolvent techniques for the production of pharmaceutical formulations with enhanced oral bioavailability.

Keywords: Microparticles; Dense antisolvent precipitation; Phenytoin; Bioavailability; Solid dispersion

1. Introduction

An increasing number of new chemical entities emerging from drug discovery and reaching drug development are poorly or very poorly water soluble, i.e., their equilibrium solubility in water is below 100 or below 10 μg/ml, respectively. Therefore, there is a great interest in the pharmaceutical industry to develop reliable, efficient, and scalable methods to increase the oral bioavailability of poorly water-soluble compounds. Classical approaches to tackle this challenge include salt formation, solubilization, and size reduction, which all suffer from more or less severe drawbacks (Serajuddin, 1999). Size reduction by micronization is probably the most commonly used approach, but there are practical limits to how much size can be reduced by conventional milling and grinding methods such as dry and wet milling, or high pressure homogenization. Classical direct particle formation processes such as controlled crystallization or precipitation hardly ever match the particle size distribution (PSD) requirements for bioavailability enhancement to be effective directly, thus necessitating an additional comminution step. Some of the most severe drawbacks related to the above processes may be overcome by either generating micronized drug particles in a robust single-step process directly, or by forming a so-called solid solution or solid dispersion of the poorly water-soluble drug in a hydrophilic carrier (Serajuddin, 1999). The concept of solid dispersions was originally proposed by Sekiguchi and Obi, who investigated the generation and dissolution performance of eutectic melts of a sulfonamide drug and a water-soluble carrier in the early 1960s (Sekiguchi and Obi, 1961). In such a formulation, the drug is typically dispersed molecularly in a polymer matrix, and released in form of colloidal particles in the gastrointestinal tract upon exposure to an aqueous medium and disintegration of the tablet or capsule, thus greatly enhancing the dissolution rate by surface enlargement. However, the number of commercial products marketed as solid dispersions still remains rather limited due to unresolved issues in the methods of preparation, particularly poor reproducibility of the processes and of the physico-chemical properties of the

* Corresponding author. Tel.: +41 44 6322456; fax: +41 44 6321141.
E-mail address: marco.mazzotti@ipe.mavt.ethz.ch (M. Mazzotti).

0378-5173/$ – see front matter © 2005 Elsevier B.V. All rights reserved.
doi:10.1016/j.ijpharm.2005.10.026

products, as well as poor physical and chemical stability of the drug–matrix complex (Serajuddin, 1999).

Compressed gas antisolvent precipitation is able to follow both promising routes for oral bioavailability enhancement of poorly water-soluble compounds discussed above, i.e., direct micronization of pure drug compounds, and co-formulation of poorly soluble drug compounds with water-soluble carriers into solid dispersions (Perrut et al., 2005a,b). In particular, the gas antisolvent recrystallization (GAS) and precipitation with a compressed antisolvent (PCA) processes rank among the most promising methods of particle formation using compressed fluids, especially in the area of pharmaceutical compounds. This is due to their favorable properties such as mild and inert operating conditions, high product quality, very low residual solvent content, sound particle size and morphology control, as well as process robustness and scalability. Supercritical antisolvent precipitation has been introduced in the late 1980s and early 1990s, and experimental proofs of concept are abundant in the scientific literature for a plethora of model compounds from very different areas such as drugs and pharmaceutical compounds, polymers and biopolymers, explosives and energetic materials, superconductor and catalyst precursors, dyes and biomolecules such as proteins and peptides, among others. These have been recently and thoroughly reviewed (Jung and Perrut, 2001; Shariati and Peters, 2003; Foster et al., 2003), and here we will only briefly review the available scientific literature on drug–polymer co-precipitation using compressed gases as antisolvents.

From the very beginning of supercritical fluid particle generation research, the formation of biocompatible polymer and drug-loaded biopolymer microparticles for pharmaceutical applications has been studied intensely by a number of research groups. Historically, most of the co-formulation applications investigated were matrix-type controlled drug release systems, which were again mostly intended for use as implants or as injectable microparticles following the parenteral route rather than for oral bioavailability enhancement of poorly soluble compounds. Conceptually, in these applications pharmaceutical agents were to be slowly released from the formulations by diffusion of the drug through the polymer matrix, or by erosion of the polymeric shell. Obviously, biopolymers degrade to non-toxic products in vivo, and surgical removal of an implant or a depot type formulation is not required after the drug reserve is consumed.

In the early 1990s, Randolph et al. first applied the PCA spray process to the precipitation of biopolymers, and formed L-PLA micro- and nanoparticles from methylene chloride using CO_2 as antisolvent (Randolph et al., 1993). Their early results were extended by Johnston and co-workers, who efficiently controlled product morphology by variations of the operating parameters (Bodmeier et al., 1995). The same group later studied the effect of nozzle type and design on product quality for various model polymers, including again L-PLA (Mawson et al., 1997). Coaxial nozzles were reported to have the most favorable characteristics for PCA operation, and markedly reduce the extent of agglomeration in the product. Other biopolymers investigated extensively include dextran and poly(hydroxypropyl methacrylamide) (HPMA) (Reverchon et al., 2000), hyaluronic acid benzylic ester (Elvassore et al., 2001), DL-PLG and DL-PLA (Bleich et al., 1993; Ruchatz et al., 1997; Ghaderi et al., 1999), and polycaprolactone (Ghaderi et al., 1999).

Following the first co-precipitation experiments of a drug and a polymer in the rapid expansion of supercritical solutions (RESS) process reported by Debenedetti et al. in the early 1990s (Debenedetti et al., 1993), research efforts towards the generation of controlled drug release formulations using dense gas processes have multiplied. Johnston and co-workers jointly entrapped water-soluble chlorpheniramine maleate and water-insoluble indomethacine in L-PLA microparticles using the PCA process (Bodmeier et al., 1995). Spherical particles in the size range of 1–5 μm were generated, but encapsulation efficiencies were rather low, especially for the poorly water-soluble compound. This effect was attributed to the partitioning of both drugs into the external CO_2 phase, and to drug extraction from the microspheres during the drying step (Bodmeier et al., 1995). Insulin-loaded polymeric nano- and microparticles generated by PCA have also been reported (Elvassore et al., 2001a,b). In fact, L-PLA particles containing insulin and poly(ethylene glycols) were produced from a mixture of DMSO and methylene chloride, and encapsulation efficiencies of up to 90% along with high hypoglycemic activities upon PCA processing were observed. However, release studies revealed that only a little amount of drug was actually released from the formulations (Elvassore et al., 2001a,b). The preparation of biodegradable beads impregnated with gentamycin for the treatment of osteomyelitis has been studied extensively by Randolph and co-workers (Falk et al., 1997; Meyer et al., 1998; Dernell et al., 2001). Gentamycin, naloxone, and naltrexone were solubilized in methylene chloride, and then processed using the PCA process. Composite particles were spherical in shape and submicron in size at rather high gentamycin loadings. Low burst effects along with linear release kinetics were obtained, indicating matrix diffusion control of drug release (Falk et al., 1997). No significant change in release kinetics was observed upon sterilization, and the PCA-processed L-PLA beads continued to release drug for over 4 months in vitro (Meyer et al., 1998). An in vivo test in sheep has also been reported (Dernell et al., 2001).

Additional studies include the incorporation of hyoscine butylbromide in L-PLA (Bleich et al., 1994), as well as of indomethacine, piroxicam, and thymopentin in L-PLA (Bleich and Müller, 1996), of tetracosactide in L-PLA (Bitz and Doelker, 1996), and of hydrocortisone in DL-PLG (Ghaderi et al., 2000).

In the area of bioavailability enhancement of poorly water-soluble compounds, the number of applications of compressed fluid antisolvent precipitation available in the scientific literature remains rather limited (Perrut et al., 2005b). Among these, Kikic and co-workers have co-precipitated carbamazepine with PEG 4000 using the GAS process, and observed increased dissolution rates of the composite particles compared to pure, micronized carbamazepine (Moneghini et al., 2001); dissolution rates increased with increasing polymer content in the composite particles, as expected (Moneghini et al., 2001).

Meure et al. have co-precipitated copper-indomethacine with poly(vinyl-pyrrolidone) using a modification of the PCA process, thereby forming a new complex, which showed considerably higher dissolution rates compared to factory grade

copper-indometahcine and PVP-indomethacine physical mixtures (Meure et al., 2004). The formation of solid solutions of a model drug and either Eudragit 100 (a polymer) or mannitol by means of a modified PCA process was studied by Juppo et al. (2003). While in the case of co-precipitation with mannitol the formation of true solid solutions failed, in the case of Eudragit a real solid solution was obtained. However, the yield was reported to be very low, due to the physicochemical properties of the polymer (Juppo et al., 2003).

In this work, we aim at systematically elucidating the potential of the gas antisolvent and precipitation with compressed antisolvent processes to enhance the dissolution behavior of poorly water-soluble drugs by investigating the micronization of neat drug substance on the one hand, and the generation of drug–polymer co-formulations on the other. We analyze the effect of process parameters on process performance and product quality for both processes, and critically compare PCA processed co-formulations to spray-dried composite particles.

2. Material and methods

Phenytoin (5,5-diphenyl hydantoin, $C_{15}H_{12}N_2O_2$; Sigma–Aldrich, Buchs, Switzerland, 99%), poly(vinyl-pyrrolidone) with a molecular weight of about 40 kDa (PVP-K30; Fluka, Buchs, Switzerland, purum), acetone (J.T. Baker, Deventer, The Netherlands, 99.5%), ethanol (J.T. Baker, absolute), and CO_2 (PanGas, Schlieren, Switzerland, technical grade and Carbagas, Basel, Switzerland, technical grade) were all used as received. The GAS and PCA units used in this work (and located in the laboratories of ETH Zurich and Novartis Pharma AG, respectively) and the corresponding experimental procedures are described in detail elsewhere (Muhrer and Mazzotti, 2003; Fusaro et al., 2005). The product quality of phenytoin microparticles and of drug–polymer co-precipitates has been characterized using a battery of analytical techniques. In particular, laser light diffraction was used to measure average particle sizes and particle size distributions (PSDs), and scanning electron microscopy (SEM), X-ray powder diffraction (XRD), and differential scanning calorimetry (DSC) were used to characterize particle shape, and morphology. Purity and residual solvent content were assessed using appropriate HPLC and GC methods, and the phenytoin content in the co-formulations was qualitatively detected and quantified by means of Raman and UV spectroscopy, respectively. Finally, intrinsic dissolution rate measurements were carried out to quantitatively compare the dissolution behavior and performance of the pharmaceutical formulations generated in this work.

2.1. Characterization of particle size, shape, and morphology

Where appropriate, a Sympatec Helos laser light diffraction particle sizer (Sympatec GmbH, Clausthal-Zellerfeld, Germany) was used to measure the product PSDs, and pure phenytoin samples were typically suspended in 50 ml of demineralized water containing approximately 0.1% (v/v) of the non-ionic tenside Tween 20 (poly(ethylene glycol)-sorbitan-monolaureate; Fluka, Buchs, Switzerland). No ultrasonication was applied in order to avoid breakage of brittle, fragile crystals. When medium to high aspect ratio needles were observed in the product originating from GAS or PCA experiments, approximate needle lengths or needle length ranges were determined by image analysis of the SEM photomicrographs. Measurement of average particle size and PSD in liquid suspension was not feasible in the case of drug–polymer co-formulations due to their amphiphilic nature. In this case, a suitable liquid carrier for the PSD measurement in suspension is hardly ever identified, thus leading to the use of a dry powder particle size measurement method. In this study, the PSDs of phenytoin–PVP micro-composites was measured on a TSI Aerosizer dry powder particle sizer equipped with an Aerodisperser unit (TSI GmbH, Aachen, Germany). Shear force and feed rate were set to medium, deagglomeration was high, and pin vibration was on during the Aerosizer measurement. A Leo 1530 cold cathode field emission scanning electron microscope from Zeiss/LEO (Oberkochen, Germany) was used in this study, and samples were sputter-coated with typically about 2 nm of platinum in high vacuum using a sputter-coater prior to SEM analysis. X-ray powder diffraction patterns of the starting materials and the product powders were recorded on a Bruker AXS D8 Advance (40 kV, 40 mA) instrument (Bruker, Karlsruhe, Germany). Finally, a DSC822e differential scanning calorimeter from Mettler-Toledo (Schwerzenbach, Switzerland) was used to determine the melting points of the precipitates and to screen for solid phase transformations.

2.2. Characterization of product composition, and residual solvent content

The residual solvent content in the crystals precipitated using the GAS recrystallization method was measured on a Waters (Milford, MA, USA) HPLC chromatograph equipped with a Nucleosil 100-5 C18 HD column (Agilent, Palo Alto, CA, USA). A known amount of phenytoin crystals was dissolved in ethanol and water was used as the eluent. On the other hand, GC (Agilent 6890, Agilent) was used for phenytoin particles and co-formulations precipitated with PCA as well as for spray-dried composite particles. In the GC analysis, the oven was initially kept at 40 °C, and then heated to a final temperature of 200 °C at a rate of 20 °C min. Precipitates were dissolved in dimethylacetamide, and 1 μl samples were injected into an Agilent 19095V-423 HP-624 Special Analysis Column. The inlet was operated in split mode (split ratio 4:1) at a total flow rate of 27.4 ml/min. The residual solvent content was detected using an a FID type detector operated at 300 °C. The presence of phenytoin in the co-formulations was determined qualitatively by Raman spectroscopy (FBRM Raman R400, Mettler-Toledo, Schwerzenbach, Switzerland), and then quantified by UV absorption using a Cary spectrophotometer (Varian, Palo Alto, CA, USA). In the latter case a known amount of co-formulation was dissolved in methanol (J.T. Baker, 99.99%), and the absorbance determined at a wavelength of 254 nm. The absorbance of PVP-K30 at this wavelength had previously been found to be negligible. The concentration of dissolved phenytoin was then determined against an external standard solution.

2.3. Measurement of intrinsic dissolution rates

Intrinsic dissolution rates (IDR) were determined using a SOTAX-AT 7 Smart apparatus (SOTAX AG, Basel, Switzerland). In all dissolution measurements, 150–200 mg of formulation were pressed into pellets by applying a tabletting force of 10 kN for typically 30 s. Approximately 30 g of tris(hydoxymethyl)aminomethan (TRIS; Fluka, Buchs, Switzerland) and 50 g of sodium dodecyl sulfate (SDS; Fluka, Buchs, Switzerland) buffers were dissolved in 5000 ml of Milli-Q water ($R = 18.2\ \mathrm{M\Omega\,cm}$, TOC<20 ppb). The solution was stirred at 50 rpm, at a temperature of 37 ± 0.5 °C and a pH of about 9. Samples were collected manually at intervals of 15 min, and the UV absorption at 254 nm (Spectrophotometer Uvikon 810, Uvikon, Bunnik, The Netherlands) was measured. The amount of dissolved phenytoin was determined against an external standard solution.

3. Precipitation of phenytoin microparticles

3.1. GAS recrystallization experiments

Phenytoin was precipitated from its acetone solution in 11 GAS recrystallization experiments using compressed carbon dioxide as antisolvent. This investigation primarily aimed at further elucidating the effect of the specific antisolvent addition rate on size and habit of the precipitated particles.

Our group has worked out three typical patterns of behavior in terms of the effect of the specific antisolvent addition rate on product quality in the case of different pharmaceutical compounds. In particular, the specific CO_2 addition rate, Q_A, was successfully used to control the average particle size of a proprietary Novartis drug compound between 0.3 and 10 μm (Müller et al., 2000; Muhrer et al., 2003). In this context, we define Q_A as the ratio of the rate of antisolvent addition, M_A, and the amount of starting solution, M_0. In contrast, no such effect of Q_A on the average size of the precipitate particles was observed in the case of the peptide lysozyme, where particles were around 250 nm at all operating conditions investigated (Muhrer and Mazzotti, 2003). Finally, in the case of paracetamol, a strong effect of Q_A on the average crystal size was again observed (Fusaro et al., 2004). In agreement with the observations for the proprietary compound, Q_A was used to control the average particle size between 90 and 250 μm at high and low values of Q_A, respectively. However, whereas bimodal particle populations were observed at intermediate values of Q_A in the case of the Novartis compound, no such effect was found for paracetamol (Muhrer et al., 2003; Fusaro et al., 2004).

These peculiar differences in terms of effect of the specific antisolvent addition rate were explained through a detailed mathematical model of the GAS process accounting for primary and secondary nucleation, as well as particle growth. The model analysis revealed that the three typical patterns of behavior observed experimentally in terms of effect of Q_A may be explained by the interplay of primary and secondary nucleation, or the predominance of either one of the two, respectively (Muhrer et al., 2002).

Straightforwardly, increasing Q_A increases the attainable supersaturation in the system, thus creating a larger number of small particles by primary homogeneous nucleation. In most technical applications however, the formation of a new solid phase from a supersaturated mother liquor is more likely to start from foreign particles present in the solution, i.e., via heterogeneous nucleation that can occur at supersaturation levels lower than those required for primary homogeneous nucleation. Clearly, it appears rather difficult to judge whether homogeneous or heterogeneous nucleation govern a precipitation process, particulary in the case of GAS recrystallization. However, if we assume heterogeneous nucleation to be controlling a precipitation process, we may expect the nucleation rate, and thus also the product particle size, to be less pronouncedly dependent on the supersaturation level (Söhnel and Garside, 1992).

Details about the experimental program for phenytoin and the major operating parameters are summarized in Table 1. In particular, Table 1 specifies the solvent used, the specific CO_2 addition rate, Q_A, the initial amount of solvent loaded into the precipitator M_0, the antisolvent addition rate M_A and the phenytoin concentration in the starting solution, c_{phen}. The volume of the precipitator V_{prec}, the operating temperature, T, the stirring rate, n, and the initial solution saturation ratio, S_0, defined as the actual over the saturation concentration, were kept constant at 400 ml, 30 °C, 400 rpm, and 0.75, respectively, in all 11 experiments. Moreover, it is worth noting that in GAS recrystallization, compressed gas is added to the precipitator initially containing the organic solution at p = 1 atm. The pressure then rises dynamically at a rate that is dictated by the CO_2 addition rate. The experiment is stopped when the liquid is in the vessel is fully expanded. For the system under investigation, final pressures are typically around 85–90 bar. Table 1 is sorted in ascending order of values of Q_A. In the last five runs of Table 1, the effect of the organic solvent used in the experiments on product quality was explored. Ethanol and mixtures of ethanol and acetone were additionally investigated, since it had previously been demonstrated that the nature of the solvent may have a substantial effect on size, shape, and morphology in GAS recrystallization (Müller et al., 2000; Muhrer et al., 2003).

3.1.1. Effect of the specific antisolvent addition rate

Let us discuss the effect of the specific CO_2 addition rate on the average size of the phenytoin crystals by examining runs G1–G7 in Table 1. The initial amount of solution, M_0, and the antisolvent addition rate M_A were chosen such as to cover a range of the specific antisolvent addition rate, Q_A, spanning over more than an order of magnitude, i.e., between 0.07 and 2 $\mathrm{min^{-1}}$. In runs G1–G4, rather large solvent amounts (i.e., 60 g in runs G1, G2, and G4, and 50 g in run G3) were used in order to investigate the lower Q_A region. The corresponding SEM photomicrographs are illustrated in Fig. 1a–d, and give two important indications. First, the average crystal size and volume markedly decrease when Q_A is increased from 0.07 to 0.5 $\mathrm{min^{-1}}$, which has been confirmed in the corresponding particle size measurements. Secondly, rhombic crystals are obtained in runs G1 and G2, whereas crystals with a columnar habit are formed in runs

Table 1
Operating conditions of the GAS precipitation experiments with phenytoin

Run	Solvent	c_{phen} (wt.%)	M_0 (g)	M_A (g/min)	Q_A (min^{-1})	Shape
G1	Acetone	3	60	4	0.07	a
G2	Acetone	3	60	6	0.1	a
G3	Acetone	3	50	10	0.2	a, (b)
G4	Acetone	3	60	30	0.5	(a), b
G5	Acetone	3	25	30	0.5	(a), b
G6	Acetone	3	25	25	1	b
G7	Acetone	3	25	50	2	b
G8	Ethanol	1.5	50	25	0.2	–
G9	25% e/a	4.6	50	25	0.2	–
G10	50% e/a	4.6	50	25	0.2	–
G11	75% e/a	3.3	50	25	0.2	–

In the second column *x*% e/a means *x* volume of ethanol in acetone. In the last column 'a' indicates the prevalence of rhombic crystals; 'b' the prevalence of columnar crystals

G3 and, most evidently, in run G4. This size reduction and morphological transition from rhombic to columnar shape is even more evident in runs G6 and G7 illustrated in Fig. 1e and f. In these runs, M_0 had been reduced to 25 g in order to reach values of Q_A between 0.5 and 2 min^{-1}. The reproducibility of the above effect has been duly checked in run G5, and as expected, the particles had the same characteristics as those in run G4 (not shown).

As the solute concentration in the starting solution, and thus the initial saturation ratio S_0, was kept constant in all 11 experiments, the decrease of particle volume is attributed to a higher value of the nucleation rate. As it is outlined above, this is in sound agreement with previous theoretical and experimental investigations, which had demonstrated that in systems governed by primary nucleation, Q_A controls the attainable supersaturation, and thus the final particle size (Fusaro et al., 2004; Muhrer et al., 2002).

It is worth keeping in mind at this point that high supersaturation levels at high values of $Q_A = M_A/M_0$ may also influence the relative growth rates among crystal faces. Such an effect was recently observed for paracetamol (Fusaro et al., 2004), and our phenytoin data summarized in Table 1 and Fig. 1 exhibit a similar trend.

3.1.2. Effect of the solvent

It is well known that in conventional crystallization processes the nature of the solvent may have a decisive effect on the final product quality. Not surprisingly, similar observations have been reported for GAS precipitation (Müller et al., 2000). In the present investigation, the effect of the solvent was studied in runs G8–G12, where ethanol and ethanol/acetone mixtures were used as alternative solvents beside pure acetone. In these experiments V_{prec}, T, n, Q_A, M_0, and S_0 were kept constant at 400 ml, 25 °C, 400 rpm, 0.2 min^{-1}, 50 g, and 0.75, respectively. As illustrated in Fig. 2, particle shape becomes increasingly elongated with increasing ethanol content. Finally, when pure ethanol is used, very fine, high aspect ratio needles are obtained. It is worth noting that though very different in shape and appearance, the particles still have the same crystal form as confirmed by XRD and DSC analysis.

3.2. PCA precipitation experiments

The PCA process was also used to precipitate phenytoin from its acetone solution in a series of 10 experimental runs. More precisely, the operating parameters in the experiments were chosen such as to assess the effect of pressure, temperature, solution concentration, and ratio of the CO_2 and solution flow rates on product characteristics. It is worth noting that phenytoin precipitated in the form of fine, medium to high aspect ratio needles at all operating conditions investigated, this particular habit being typically associated to very high supersaturation levels.

Mass transfer is faster and more efficient in PCA than in GAS (Lin et al., 2003; Fusaro et al., 2005). Both GAS and PCA precipitation are governed by the same mechanisms of particle formation and growth, but feature markedly different mass transfer time constants, PCA reaching larger mass transfer rates and supersaturation levels than GAS (Fusaro et al., 2005; Lin et al., 2003). In the analysis of the GAS data above, we had assumed that the relative growth of the faces of phenytoin crystals is strongly influenced by the evolution of the supersaturation during the process. The fact that needle-like particles are obtained in PCA experiements, where supersaturations are considerably higher than in GAS, is fully consistent with this conclusion.

It is worth mentioning that also in this case, the morphological transition was not associated to any change in the crystal form, as confirmed by XRD and DSC analysis. However, crystal shape is identified as a sensitive indicator for the precipitation conditions adopted in an experiment, as outlined below. All PCA experiments are summarized in Table 2, where pressure, p, temperature, T, phenytoin concentration in absolute units, c_{phen}, and in terms of saturation ratio, S_0, as well as the solution and antisolvent flow rates, M_{sol} and M_A, are listed. In the rightmost column of Table 2, qualitative precipitate characteristics from the image analysis of SEM photomicrographs are given. The effect of temperature and pressure is investigated in runs P1–P5, the effect of the flow rate ratio, M_A/M_{sol} in runs P4, P6, and P7, the effect of initial solution concentration (or initial saturation ratio) in runs P1 and P8, P6, P9, and P10. The residual acetone content in the product is not explicitly mentioned in Table 2,

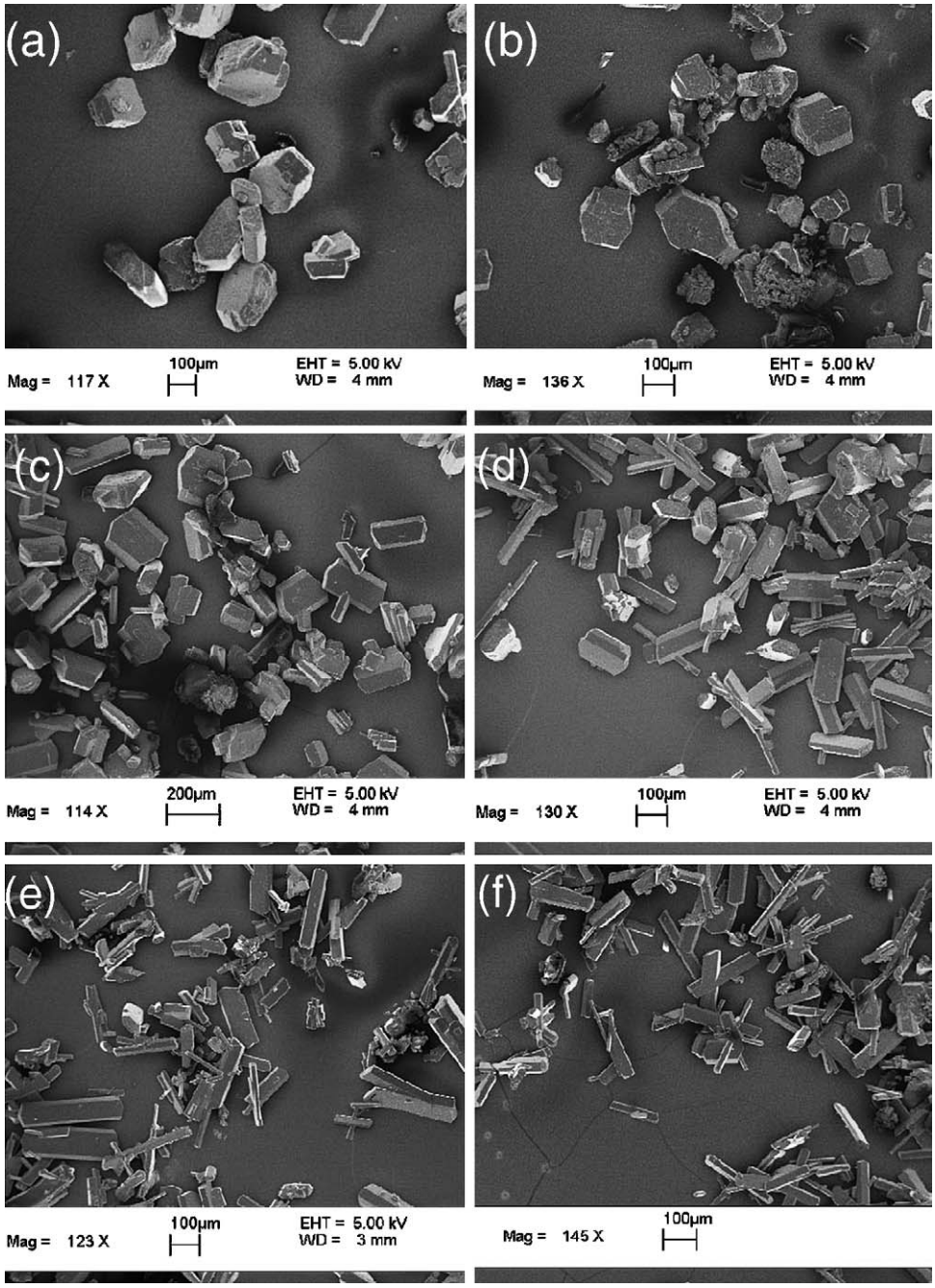

Fig. 1. Effect of Q_A at 30 °C, $S_0 = 0.75$ and stirring rate $n = 400$ rpm. SEM photomicrographs of particles precipitated in: (a) run G1 at $Q_A = 0.07\,min^{-1}$; (b) run G2 at $Q_A = 0.1\,min^{-1}$; (c) run G3 at $Q_A = 0.2\,min^{-1}$; (d) run G4 at $Q_A = 0.5\,min^{-1}$; (e) run G6 at $Q_A = 1\,min^{-1}$; (f) run G7 at $Q_A = 2\,min^{-1}$.

but has been routinely checked for all samples and found to be always below 150 ppm.

3.2.1. Effect of temperature and pressure

Let us first consider experimental runs P3–P5 in Table 2, where the pressure was varied between 95 and 150 bar while keeping the temperature constant at 50 °C, and the SEM photomicrographs of the corresponding product particles in Fig. 3. In our experiments at 150 bar (run P5) and 120 bar (run P4), high aspect ratio needles are formed as shown in Fig. 3a and b, respectively. On the contrary in run P3 at $p = 95$ bar, as shown in Fig. 3c, the morphology of the precipitate changes rather dramatically, as the experimental point approaches the mixture critical point; the product appears in fact as agglomerates of roughly spherical, fused particles, containing some columnar crystals.

As shown in Fig. 4, at a temperature of 50 °C the critical point of the acetone–CO_2 binary mixture is at about 90 bar (Adrian and Maurer, 1997), hence under the wide pressure range adopted in runs P3–P5, the phase behavior of the solvent–antisolvent mixture changes rather dramatically. In the supercritical mixture region due to the vanishing of interfacial tension and the fact that solvent and antisolvent become fully miscible, fluid mix-

Table 2
Operating conditions of the PCA experiments with phenytoin and precipitate characteristics

Run (°C)	T (°C)	p (bar)	c_{phen} (wt.%)	S_0(−)	M_A (g/min)	M_{sol} (ml/min)	Product quality
P1	30	90	4	1	80	1	Medium aspect ratio needles in the 20–50 μm range; lath-shaped particles in the 30–60 μm range; agglomerates
P2	40	100	4	0.89	80	1	High aspect ratio needles, length up to 220 μm; lath-shaped particles in the 1–150 μm range; large agglomerates
P3	50	95	4	0.77	80	1	Irregular and columnar particles in the 1–12 μm range; 2 μm in thickness
P4	50	120	4	0.77	80	1	Medium aspect ratio needles in the 20–90 μm range; few small aggregates formed by needles and lath-shaped particles
P5	50	150	4	0.77	80	1	High aspect ratio needles, length up to 220 μm; laths in the 1-150 μm range and aggregates of lath-shaped particles
P6	50	120	4	0.77	60	1	High aspect ratio needles, length up to 200 μm; strong agglomeration
P7	50	120	4	0.77	80	0.5	Medium aspect ratio needles in the 5–100 μm range; columnar particles around 50 μm
P8	30	90	3	0.75	80	1	Medium to high aspect ratio needles in the 20–250 μm range
P9	50	120	2	0.38	80	1	Medium to high aspect ratio needles in the 20–250 μm range
P10	50	120	3	0.58	80	1	Medium to high aspect ratio needles in the 20–180 μm range; most below 50 μm

ing rather than jet break-up into droplets becomes the controlling mechanism for particle formation (Lengsfeld et al., 2000; Shekunov et al., 2001a). Dukhin et al. have in fact demonstrated that when ethanol is injected into compressed CO_2 two flow regimes can be observed depending whether the pressure is lower or higher than the critical pressure of the binary mixture at the temperature of the experiment. In the former case, the solution is atomized into droplets, whereas in the latter case, i.e., in the supercritical region, a gas-like jet is observed (Dukhin et al., 2003).

For the particle formation mechanism, this means that in the subcritical and near-critical case nucleation and growth of the particles are likely to be confined into the solvent rich droplets forming when the solution is contacted with the antisolvent. On the other hand, in the supercritical case, nucleation and growth take place in the gas-like jet as soon as the solution and the antisolvent streams are mixed intensely enough to create supersaturation. Moreover, in the supercritical region, fast mass transfer between solution and antisolvent and achievement of higher supersaturation levels than in the near critical and subcritical region are favored, as rapid turbulent mixing rather than molecular diffusion through the droplet interface is the controlling mechanism for mass transfer Shekunov et al. (2001a,b). Fig. 4 clearly shows how the distance between the experimental pressure and the critical pressure progressively increases in runs P3–P5, moving the experimental point from the sub- or near critical two-phase region into the supercritical one-phase region, thus affecting the fluid flow regime. Therefore, similarly to earlier results on paracetamol (Fusaro et al., 2005), we consider such distance responsible for the different fluid flow regimes accessed in runs P3 (droplet formation) and P4–P5 (gas-like jet), hence for the difference in product quality illustrated in Fig. 3. Likewise, in the case of run P2 particles with characteristics rather similar to those in runs P4 and P5 are found; though carried out at a similar pressure (100 bar) as run P3, due to the lower experimental temperature (40 °C), the distance of the experimental point from the critical pressure is in the same order as for run P4.

3.2.2. Effect of the flow rate ratio

In the PCA process, the ratio between the flow rates of the solution and of CO_2 controls the supersaturation level that can be reached in the injection device. The effect of varying the flow rate ratio on product quality has been investigated in runs P4, P6, and P7 at 50 °C, 120 bar, and a solute concentration, c_{phen}, of 4 wt.%. M_A to M_{sol} ratios of 60:1, 80:1, and 160:1 were studied by setting the CO_2 flow rate to values between 60 and 80 g/min, and the solution flow rate to values between 0.5 and 1 ml/min, accordingly. Following the argument in Section 3.2.1, in this region of the operating parameter space, we expect particle formation to be controlled by mixing rather than by jet break-up into droplets. Let us first inspect run P6 carried out at the lowest flow rate ratio of 60:1. The corresponding SEM photomicrograph in Fig. 5a shows mostly high aspect ratio needles with needle lengths of up to 200 μm, which is very similar to the results of run P4, where the flow rate ratio was 80:1. The effect of the flow rate ratio on product quality becomes evident in Fig. 5b, where particles obtained in run P7 are shown. It is readily observed that increasing M_A relative to M_{sol} yields a particulate product containing both needles and columnar crystals. Columnar particles from run P7 are rather similar to the morphology of particles recrystallized by GAS at very high values of the specific CO_2 addition rate.

3.2.3. Effect of the initial concentration

The effect of phenytoin concentration in the starting solution has been studied in two series of runs at 30 °C/90 bar (runs P1 and P8), and 50 °C/120 bar (runs P4, P9, P10), respectively. At 120 bar, c_{phen} was varied between 2 and 4 wt.%, corresponding to an S_0 range of 0.38 to 0.77. Needles of up to 200 μm in length are formed at a low initial saturation ratio of 0.38 in run P9, as

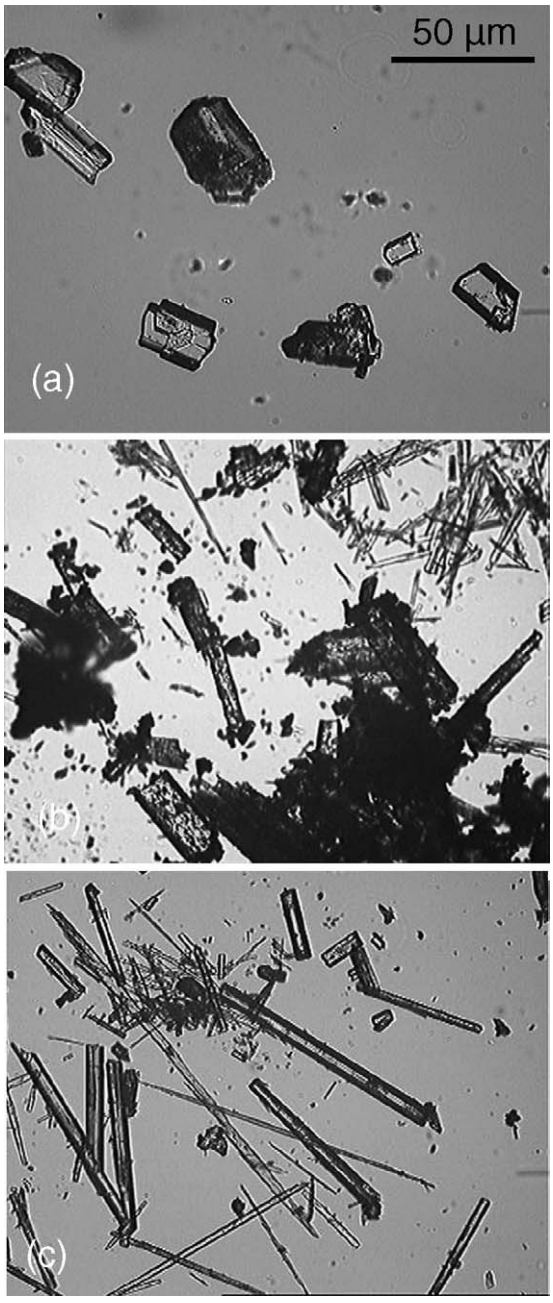

Fig. 2. Effect of the solvent on the morphology of phenytoin crystals precipitated at 30 °C, $S_0 = 0.75$, stirring rate $n = 400$ rpm and $Q_A = 0.2\ \text{min}^{-1}$ in: (a) run G3 from acetone; (b) run G11 from a 75%/25% volumetric ethanol/acetone mixture; (c) run G8 from ethanol.

illustrated in Fig. 6a. When the initial saturation ratio is increased to a value of $S_0 = 0.58$ in run P10, we observe a decrease of the needle length, a marked increase in the extent of agglomeration and the presence of platelet-like particles (Fig. 6b). The overall product quality in run P10 is thus again similar to run P4 at $S_0 = 0.77$. The observation that agglomeration extent tends to increase at higher solution concentrations is hardly surprising, and confirmed at a lower operating pressure of 90 bar for initial saturation ratios of 0.75 and 1 in runs P8 and P1, respectively. As readily observed in Fig. 6c, needles are in fact formed at $S_0 = 0.75$ in run P8, whereas the particles precipitated from a saturated solution are highly agglomerated, exhibiting a fused, surface, and an increased content of plate-like crystals (Fig. 6d).

4. Formation of phenytoin/PVP solid dispersions

Let us consider the formation of drug–polymer co-formulations of phenytoin and PVP-K30 by compressed fluid antisolvent precipitation and by convenstional spray drying. In particular, we investigate the potential of both the GAS and PCA processes for generating solid dispersions of poorly water-soluble compounds in water-soluble polymeric carriers, and compare the in vitro dissolution behavior of particles obtained in this manner to spray-dried solid dispersion particles.

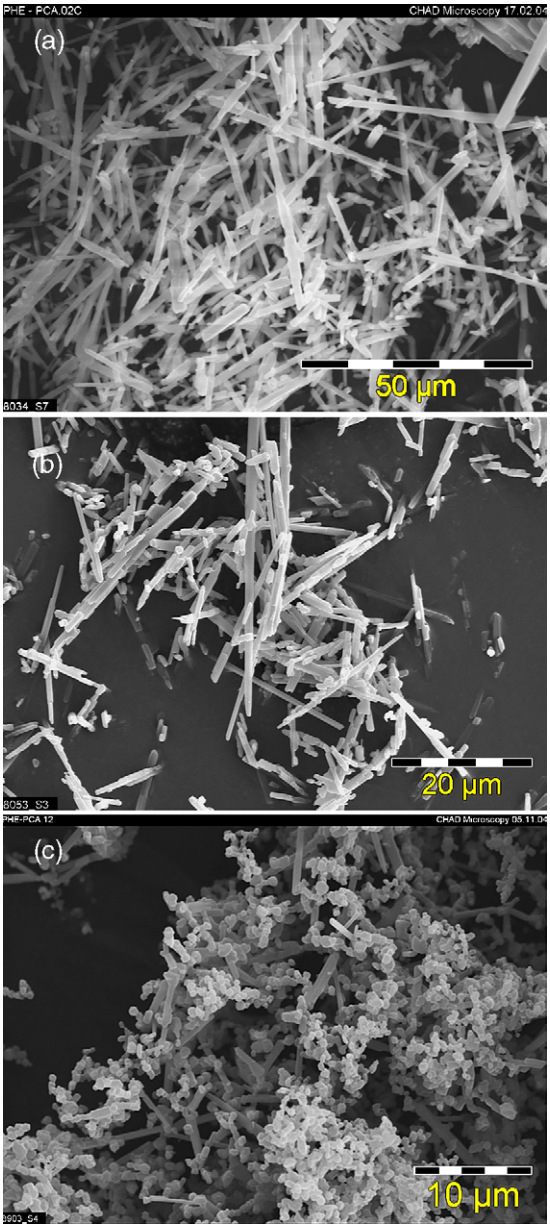

Fig. 3. Effect of pressure on phenytoin crystals precipitated with PCA : (a) run P5 at 150 bar (magnification 1000:1); (b) run P4 at 120 bar (1500:1); (c) run P3 at 95 bar (2500:1).

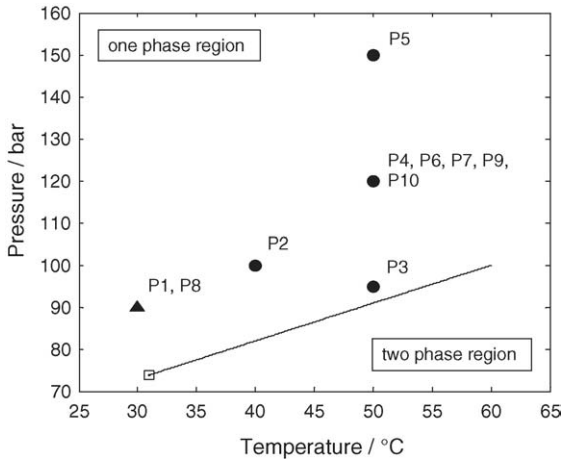

Fig. 4. Location of the PCA experiments with phenytoin with respect to the projection of the critical loci of the CO_2–acetone binary system into the p–T plane. (●) Experiments carried out at supercritical conditions; (▲) experiments carried out at subcritical conditions.

In a first attempt, the GAS recrystallization of PVP-K30 from ethanol/acetone mixtures, and methylene chloride was studied. Initial concentration, operating temperature, and specific CO_2 addition rate were varied between 0.5 and 8 wt.%, 5 and 30 °C, and 0.5 and 2 min^{-1}, respectively. However, liquid–liquid phase separation was observed prior to vitrification of the polymer-rich phase at all conditions investigated, typically yielding large, porous, interconnected polymer structures rather than discrete particles. This is a rather common feature in the GAS recrystallization of polymeric systems, by and large due to mass transfer effects (Bungert et al., 1998). Therefore, we have concluded that

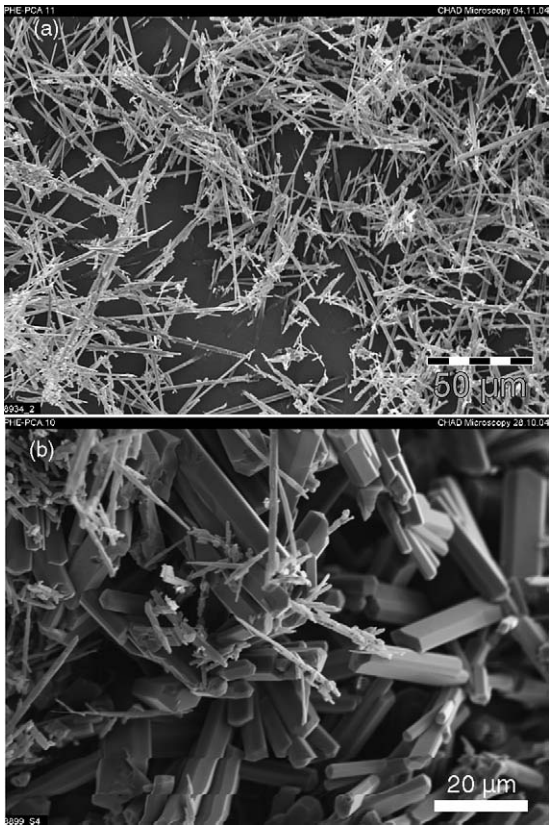

Fig. 5. Effect of the CO_2 to solution flow rate ratio on phenytoin particles precipitated with PCA in: (a) P6 at M_A to M_{sol} ratio of 60 (magnification 450:1); (b) run P7 at M_A to M_{sol} ratio of 160 (1000:1).

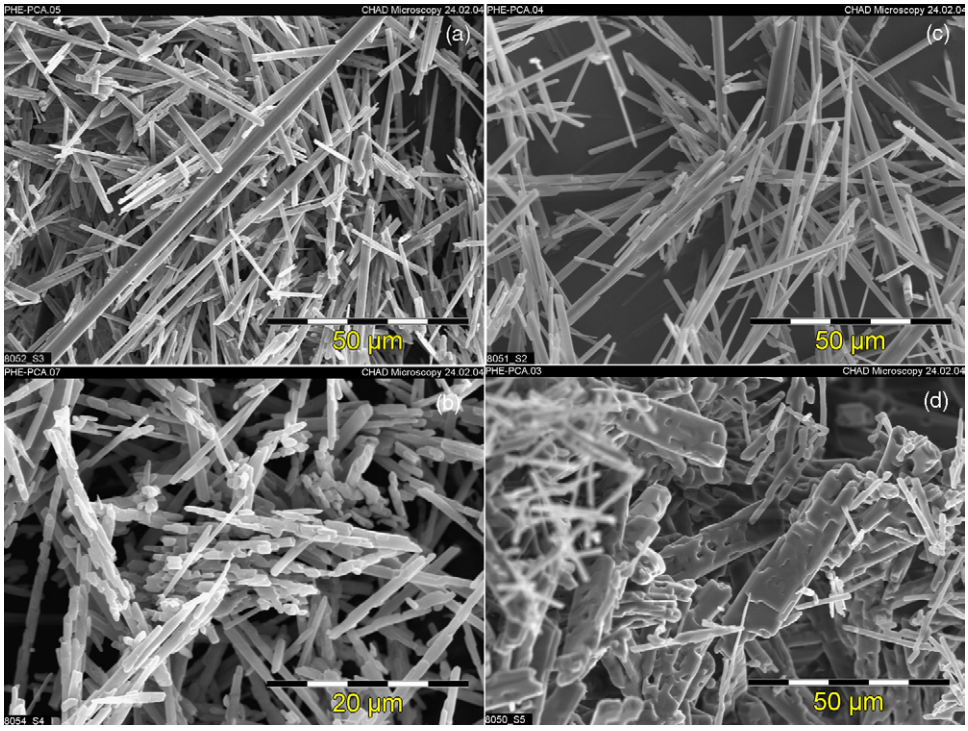

Fig. 6. Effect of concentration on phenytoin particles precipitated with PCA in: (a) run P9 at $S_0 = 0.38$ (magnification 1000:1) $T = 50$ °C, $p = 120$ bar; (b) run P10 at $S_0 = 0.58$ (1000:1), $T = 50$ °C, $p = 120$ bar; (c) run P8 at $S_0 = 0.75$, $T = 30$ °C, $p = 90$ bar (2000:1); (d) run P1 at $S_0 = 1$, $T = 30$ °C, $p = 90$ bar (1000:1).

PVP particle formation can be successful only when a more effective solvent–antisolvent mass transfer is realized, i.e., using the PCA process.

PCA precipitation of pure PVP-K30 microparticles was indeed successful, and most conveniently an ethanol/acetone mixture (24 wt.% ethanol) was used as organic solvent phase. Previous experiments had shown that poor polymer yields were observed when PVP-K30 was precipitated from pure ethanol using the PCA process, which we attribute to an increased polymer solubility in the CO_2–ethanol binary mixture. The addition of 76% (w/w) of acetone to the solution was introduced to lower the solubility of PVP in the solvent-modified CO_2, while still dissolving appropriate amounts of phenytoin. Additionally, PVP yields were found to be highest (≥95%) when operating in the two-phase region, i.e., at pressures below the critical pressure of the binary system, namely around 80 bar and 25 °C.

4.1. PCA co-precipitation experiments

The possibility of molecularly dispersing phenytoin in a continuous matrix of poly(vinyl-pyrrolidone) to form a solid dispersion, and its effect on the in vitro dissolution performance was next assessed in a series of seven experimental runs. The main operating parameters were chosen based on the outcome of our previous PCA experiments on both pure phenytoin and PVP-K30. In particular, an ethanol/acetone mixture (24 wt% ethanol) was always used as organic solvent, and pressure and temperature were kept constant at 80 bar and 25 °C, respectively, in six of the seven runs in order to maximize product yield. The main operating parameters of the seven PCA runs are summarized in Table 3, namely the concentration of phenytoin, c_{phen}, and PVP-K30, c_{PVP}, in the starting solution, the system pressure, p, the operating temperature, T, the CO_2 addition rate, M_A, and the solution flow rate, M_{sol}. Table 3 reports also the relative amount of phenytoin present in the co-precipitate measured by UV spectroscopy, and a qualitative description of the product appearance from the SEM photomicrographs.

Clearly, composition homogeneity is a key aspect in the generation of solid dispersions or solid solutions. Taki et al. successfully entrapped the herbicide diuron in a suitable polymeric carrier using compressed gas antisolvent precipitation (Taki et al., 2001). While the compound had formed high aspect ratio needles in pure herbicide experiments, under appropriate operating conditions the active agent was successfully entrapped in the polymer. In fact, the relative concentration of active agent and polymer was reported to have a decisive influence on the encapsulation efficiency in their model system (Taki et al., 2001). Consequently, we varied the relative amounts of phenytoin and PVP-K30 in the starting solution in the range between 1:4 and 4:1 (drug to polymer) in order to get a rather comprehensive assessment of the solid–solid phase behavior of our system. In the experiments with excess polymer in the solution, i.e., at concentration ratios between 1:4 and 1:2 in runs C1–C4, the co-precipitate appeared as agglomerates of spherical primary particles, which are below 500 nm in size exclusively, i.e., no needle-like crystals were observed in the samples. This is illustrated in Fig. 7 for experiment C1, where the drug to polymer ratio was 1:4. Average particle sizes and particle size distributions from Aerosizer measurements were in sound agreement with the SEM photomicrographs in all cases.

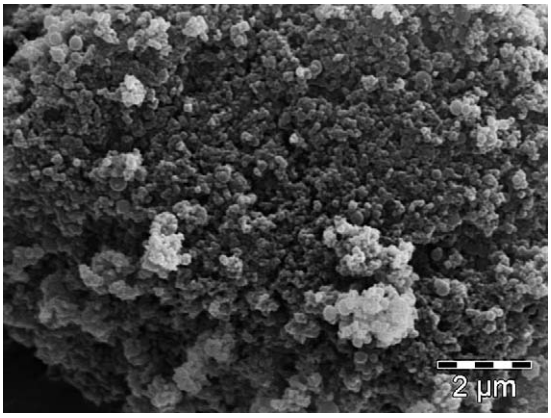

Fig. 7. Phenytoin–PVP-K30 co-formulation precipitated with PCA in run C1. The drug-to-polymer ratio was 1:4 in this case.

Solid dispersion formulations are intended to molecularly disperse and stabilize the poorly water-soluble drug compound in an amorphous state within the continuous polymeric carrier. In this study, the absence of crystalline material was routinely checked and confirmed by X-ray powder diffraction and differential scanning calorimetry. As expected, all samples precipitated with an excess of polymer in the starting solution turned out to be fully amorphous. In order to get an indication about mid-term stability also, X-ray and DSC scans of selected samples stored at 4 °C were repeated in weekly intervals for several weeks. No recrystallization of the dispersed drug substance was observed during this period, thus indicating promising stability properties. It is clear, however, that the stability of PCA processed solid dispersions under different storage conditions requires in depth investigation and assessment to be covered in future experimental work. For the sake of illustration, X-ray powder diffraction patterns of the starting material (i.e., pure phenytoin) and of co-formulation C1 are shown in Fig. 8.

Although phenytoin can not be detected by visual inspection of the SEM photomicrographs or by X-ray diffraction or

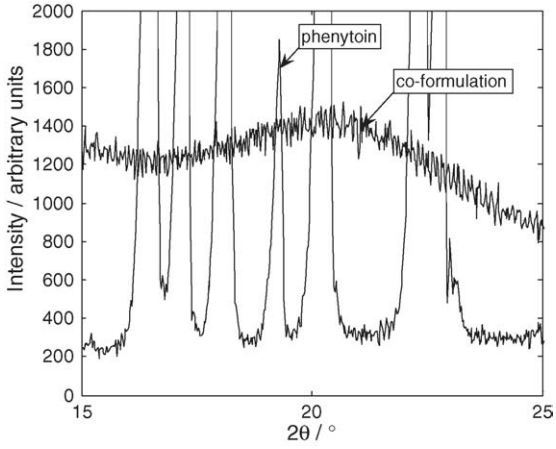

Fig. 8. Selected section of the X-ray powder diffraction patterns of pure phenytoin, and PCA co-formulation C1.

DSC, its presence in the co-precipitates has been confirmed by Raman spectroscopy. Fig. 9 shows the Raman spectra of pure phenytoin, of pure PVP-K30 and of the co-formulation C1 in the range between 1500 and 1850 cm^{-1}. It is readily observed that the co-formulation spectrum features characteristic peaks corresponding to pure phenytoin as well as to pure PVP. The combined use of Raman spectroscopy and X-ray powder diffraction thus suggests that the formation of phenytoin crystals can be successfully hindered at drug to polymer ratios smaller than 1:2. We may thus assume that phenytoin is molecularly dispersed in the polymer matrix, hence forming a true solid solution. Further investigation should aim at clarifying whether the drug is also uniformly distributed in the polymer matrix.

Quantitatively, the phenytoin content in the co-precipitate was determined by UV-spectroscopy as described in Section 2. Phenytoin contents were typically within 2% of the expected value with an excellent reproducibility (cf. runs C2 and C3 in Table 3), thus underlining the robustness of PCA precipitation. The fact that phenytoin loadings reported in Table 3 are consistently slightly above the calculated value suggests that some of the PVP is extracted from the precipitation vessel due to a non-negligible solubility of the polymer in compressed carbon dioxide at the conditions adopted. Residual solvent contents were always below 1 wt.% for both acetone and ethanol; these can be efficiently controlled and further reduced by adjusting the amount of make-up carbon dioxide flushed through the precipitation vessel during the solvent removal and drying step. In the experiments listed in Table 3, the vessel was typically flushed with about six times the vessel volume of pure CO_2. Yield (defined as the ratio between mass of product recovered and total amount of phenytoin and PVP dissolved in the starting solution) in the co-precipitation experiments was typically above 75%.

When the phenytoin content in the starting solution was increased to 2:2 or above, true solid dispersions or solutions of phenytoin in PVP were no longer formed. It appears from the SEM photomicrographs that the threshold beyond which both agglomerates of spherical primary particles and needle-like phenytoin crystals are observed in the sample lies around the 1:1 ratio. From this point onward, the amount of high aspect ratio phenytoin crystals progressively increases with increasing drug content in the starting solution, until finally, phenytoin crystals partly coated with polymer nanoparticles adhering to the crystal surface are obtained at a drug to polymer ratio of 4:1. This

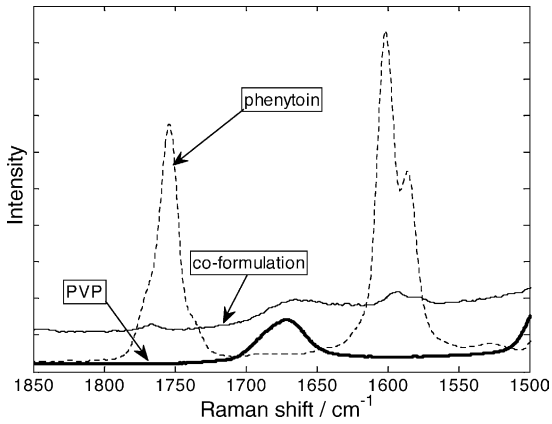

Fig. 9. Selected section of the Raman spectra of pure phenytoin, and PCA co-formulation C1.

morphological transition observed in runs C5–C7 is illustrated in Fig. 10. Although evident from Fig. 10, the effect of the drug to polymer ratio on the precipitation process and the product characteristics has to be studied further in order to elucidate the interaction of drug and excipient molecules during particle nucleation and growth of the co-precipitate, and to elucidate the mechanism hindering or fostering the formation of crystalline structures under certain operating conditions.

4.2. Spray drying experiments

Classical routes for the generation of solid dispersions mainly utilize solvent evaporation and melt crystallization processes. Melt crystallization is associated with high process temperatures which may adversely affect drug stability, and hardening and pulverization are typically very difficult to control, thus generally entailing poor reproducibility. Therefore, solvent evaporation methods have recently attracted considerable attention (Serajuddin, 1999). Clearly, there are drawbacks also here, including the use of large solvents amounts, energy-intensive processes, and often unacceptably high residual solvent contents. In this study, we use spray drying as an alternative method for the generation of phenytoin–PVP-K30 solid dispersions. This is intended to critically compare and challenge the dissolution performance of the PCA processed solid dispersions. A total of four experimental runs were carried out on a Büchi model B191

Table 3
Operating conditions of the phenytoin–PVP-K30 co-formulation experiments with PCA and product characteristics

Run	c_{phen} (wt%)	c_{PVP} (wt%)	p (bar)	T (°C)	M_A (g/min)	M_{sol} (ml/min)	x_{phen} (wt%)	Product quality
C1	0.5	2	80	25	120	0.6	19	Aggregates of spherical 200–1000 nm particles
C2	1	2	80	25	120	1.1	36	Aggregates of spherical 200–1000 nm particles
C3	1	2	80	25	120	1	35	Aggregates of spherical 200–1000 nm particles
C4	1	2	100	33	120	1	28.5	Aggregates of spherical 200–1000 nm particles
C5	2	2	80	25	120	1	–	Aggregates of 100–600 spherical particles; some needle-like phenytoin crystals
C6	2	1	80	25	120	1	–	Aggregates of needle-like phenytoin crystals entrapped in a polymer network
C7	2	0.5	80	25	120	1	–	Aggregates of needle-like phenytoin crystals with polymer adhering to the crystal surface

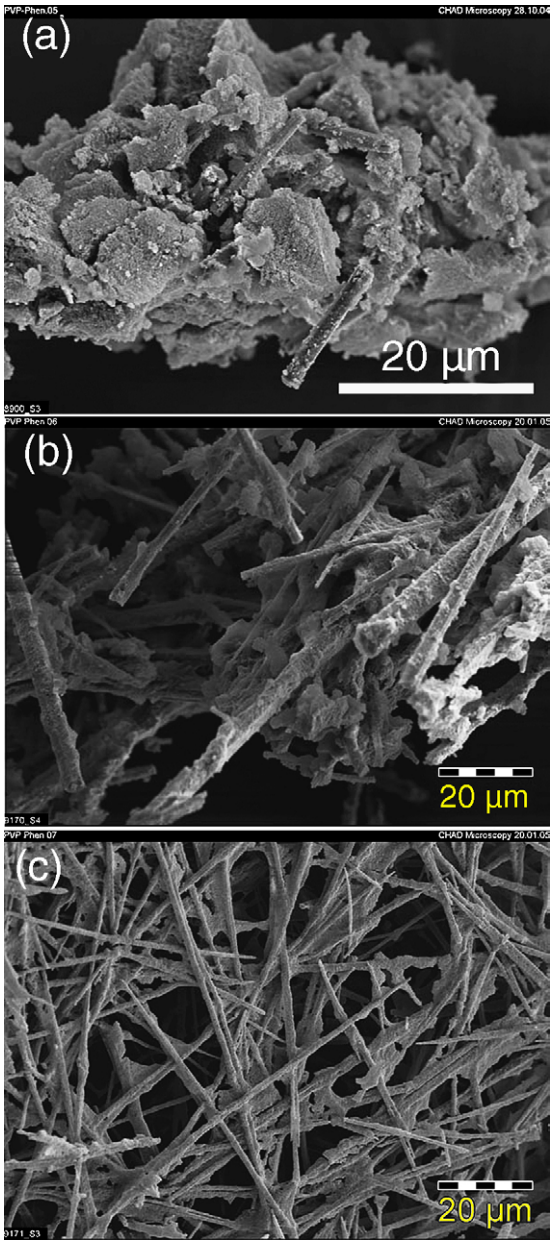

Fig. 10. Phenytoin–PVP-K30 co-formulations precipitated with PCA in: (a) run C5 at a drug-to-polymer ratio of 2:2; (b) run C6 at a drug-to-polymer ratio of 2:1; (c) run C7 at a drug-to-polymer ratio of 4:1.

Mini (Büchi, Flawil, Switzerland) laboratory scale spray drier. The drug to polymer ratios investigated were 1:2 and 1:4. Inlet temperatures were between 150 and 175 °C in all experiments, the nitrogen flow rate was 600 l/h, the atomization pressure was 4.5 bar, and the aspirator was operated at 100%. Typical experimental yields were between 54 and 68%.

4.3. Comparative analysis of dissolution performances

Intrinsic dissolution rates (IDR) were measured using a Sotax-AT7 Smart apparatus as described in Section 2. In this study, the dissolution behavior of phenytoin–PVP-K30 solid dispersions generated by PCA co-precipitation and by conventional spray drying was compared with that of pure phenytoin. Pure drug samples obtained from a PCA experiment and used as is, as well as precipitates that were further reduced in size by high pressure homogenization, were considered. For this purpose, PCA precipitates were suspended in de-ionized water containing about 0.1% (v/v) of Tween 20 and saturated with phenytoin, and then homogenized in a commercially available high pressure homogenizer (Model M-110Y, Microfluidics, Newton, MA, USA). The homogenization pressure was 1000 bar, and the particles were passed through the equipment about 10 times, typically yielding average particle sizes around 1 μm with narrow PSDs.

Table 4
Summary of the intrinsic dissolution rates IDR measured for phenytoin microcrystals and phenytoin–PVP co-precipitates

Run	IDR (mg/(cm^2 min))	Process
C1	0.191	PCA co-formulation
C2	0.148	PCA co-formulation
C3	0.177	PCA co-formulation
C4	0.157	PCA co-formulation
C5	0.133	PCA co-formulation
SD1	0.133	Spray-dried co-formulation
SD2	0.105	Spray-dried co-formulation
SD3	0.159	Spray-dried co-formulation
SD4	0.058	Spray-dried co-formulation
P3	0.025	PCA precipitated phenytoin microcrystals
H1	0.026	Micronized by high pressure homogenization

The characteristics of the powders considered, along with the results of the IDR measurements, are summarized in Table 4; five PCA co-precipitates, four spray-dried co-formulations, one pure phenytoin PCA precipitate with needle-like appearance, and one homogenized phenytoin precipitate were analyzed in the dissolution study. The intrinsic dissolution rate is defined as the slope of the curve obtained by plotting drug concentration in the buffer solution versus time, when measured during an experiment where either the drug or the drug–polymer co-formulation/solid dispersion is first tabletted (compressed into pellets) and then contacted with the stirred buffer solution. Since a specified tablet surface of known and constant area is exposed to the dissolution medium in the intrinsic dissolution rate measurement, this procedure allows to rule out any effect of particle size and PSD on the dissolution rate. Accordingly, the reported dissolution rates are then normalized by the tablet surface exposed to the dissolution medium.

We would expect samples P3 and H1 in Table 4 to feature similar intrinsic dissolution rates. And in fact, the intrinsic dissolution rates are virtually identical for the PCA precipitate and the homogenized powder at values of 0.025 and 0.026 mg/(cm^2 min), respectively, as observed in Fig. 11a. On the other hand, when phenytoin is molecularly dispersed in the water-soluble polymeric carrier to form a solid dispersion as it is the case for experiments C1–C4 in Table 4, we observe a rather dramatic effect on the dissolution performance shown in Fig. 11b. Let us first consider experiment C1, where the drug to polymer ratio is 1:4, i.e., the lowest value. In this case, an intrinsic dissolution rate of 0.19 mg/(cm^2 min) was measured, corresponding to an eight-fold increase of the rate of drug dis-

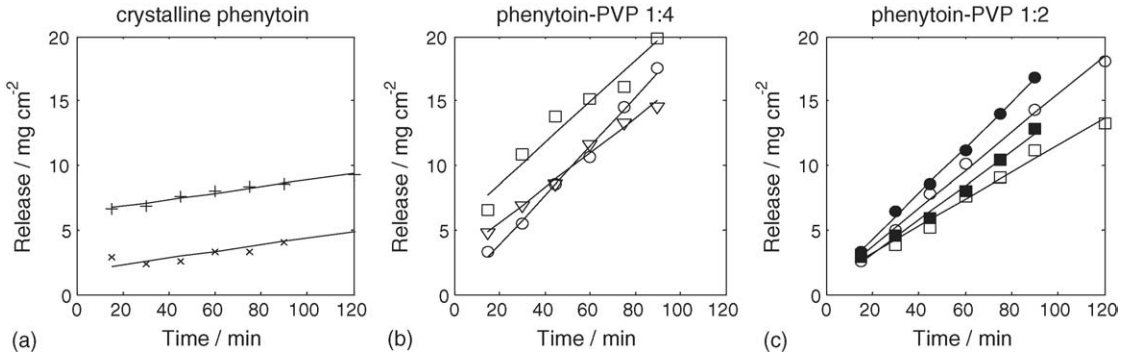

Fig. 11. Intrinsic dissolution measurements: (a) crystalline phenytoin precipitated with PCA in run P3 (+) and micronized in a high pressure homogenizer (×); (b) 1:4 phenytoin–PVP-K30 physical mixture and 1:4 phenytoin–PVP-K30 solid solutions: precipitated with PCA in run C1 (◯), spray drying exp. SD3 (□), physical mixture (▽); (c) 1:2 phenytoin–PVP-K30 solid solutions obtained by: PCA in run C2 (◯) and run C3 (●), spray drying experiments SD1 (■) and SD2 (□).

solution compared to pure phenytoin crystals. From Table 4 and Fig. 11, we observe that the in vitro dissolution performance improves with increasing polymer content as expected. The dissolution rate is highest at the lowest drug to polymer ratio of 1:4, and steadily decreases with increasing drug content. In the case of a 1:1 mixture of drug and polymer in the starting solution, a few isolated phenytoin crystals are discernible in the SEM photomicrographs reported in Fig. 10, and the dissolution rate drops sharply by almost 30%. We may also conclude from Fig. 11b that solid dispersions generated in the PCA process markedly outperform both the physical mixture and the spray-dried co-formulation at identical drug to polymer ratios. In particular, the intrinsic dissolution rate is 20 and 70% higher in the case of experiment C1, respectively. A very similar observation was made at a drug to polymer ratio of 1:2 as it is illustrated in Fig. 11c. Again, PCA-processed solid dispersions C2 and C3 outperform the spray-dried samples at identical drug to polymer ratio by up to 25%. Moreover, it is worth pointing out that the reproducibility (an absolute deviation of only 16%) is rather good in experiments C2 and C3, which were carried out at identical operating conditions and drug to polymer ratios in the initial solution. This result is particularly remarkable when compared to the spray-dried precipitates, where reproducibility is less satisfactory.

These results not only illustrate the general feasibility of compressed fluid antisolvent precipitation for the generation of solid dispersions for oral bioavailability enhancement of poorly water-soluble compounds, but also highlight process robustness and reproducibility, which are essential features for industrial consideration and application.

5. Conclusions

The use of compressed fluid antisolvent precipitation to enhance the dissolution performance of the poorly water-soluble model drug compound phenytoin has been investigated. The GAS and PCA processes have been used to generate microcrystals of neat phenytoin, and the PCA process has been applied to the generation of solid molecular dispersions of the drug in the hydrophilic carrier PVP-K30. Oral bioavailability enhancement of poorly water-soluble compounds is an important area in pharmaceutical research and development, and in spite of substantial research efforts over the past decades, the number of compounds that have reached the market as solid dispersion formulations remains very limited due to technological issues associated to the most common methods of solid dispersion generation. The number of applications of near- or supercritical antisolvent precipitation to this area reported in the scientific literature is also rather limited, and we are among the first to report a thorough investigation of process parameter effects on product quality in both the GAS and PCA precipitation of a neat drug compound, thereby elucidating similarities and differences between the two techniques, as well as an assessment of PCA performance in the generation of solid dispersions, and a critical comparison of the performance of PCA co-precipitates with spray-dried solid dispersions.

In this work, we were able to show that compressed fluid antisolvent precipitation is indeed an efficient and robust method that is capable of following both promising routes to oral bioavailability enhancement of poorly water-soluble compounds, i.e., direct micronization of pure drug compounds, and co-formulation of poorly soluble drug compounds and water-soluble carriers into solid dispersions.

In the GAS recrystallization experiments with pure phenytoin, the effect of the specific antisolvent addition rate, and the composition of the solvent were investigated. Average crystal size and volume decreased markedly at increasing values of the specific CO_2 addition rate, as it is frequently observed in GAS recrystallization. Moreover, in this case, the size reduction is associated to a morphological transition from rhombic to columnar shape, while maintaining the same crystal form. We attribute this effect to higher nucleation rates at higher values of Q_A. The effect of the solvent composition is again quite remarkable. At otherwise identical operating conditions, high aspect ratio needles are obtained in the GAS recrystallization of ethanolic phenytoin solutions, whereas compact, rhombic crystals are obtained when acetone is used. These results again demonstrate that particle size and shape is quite efficiently controlled by the governing operating parameters in GAS recrystallization.

The effect of process parameters on product quality is similarly pronounced in the PCA precipitation of phenytoin. In this case, the difference between the experimental pressure and

the critical pressure of the CO_2–acetone binary mixture at the given experimental temperature most dominantly controls product quality. In agreement with our GAS results, very high aspect ratio needles are obtained at pressures above the critical locus, whereas fused aggregates of spherical and some columnar particles are observed in the vicinity of the critical point, where particle formation possibly occurs within confined solution droplets.

Finally, the potential of PCA precipitation in the generation of drug–polymer solid dispersions has been demonstrated in a number of co-precipitation experiments. Most importantly, while the pure drug had formed high aspect ratio crystals in GAS and PCA precipitation experiments, the co-formulations were amorphous by XRD analysis, provided that the drug-to-polymer ratio was small enough, i.e., the concentration of phenytoin was small compared to the concentration of PVP-K30 in the starting solution. At drug to polymer ratios of less than 1:2, the product appeared as micron-size agglomerates of spherical nanoparticles that were completely amorphous, and showed no recrystallization tendency after several weeks of storage. As expected on the other hand, both drug crystals and polymer particles were observed at higher drug contents. The phenytoin content in the solid dispersions was within a few percent of the expected value in all cases, and the residual solvent content was also effectively controlled. Solid dispersions precipitated with PCA markedly outperformed neat drug microcrystals, physical mixtures, as well as spray-dried composite particles in in vitro dissolution experiments. The increase in the dissolution rate is up to eight-fold when compared to pure drug particles, 25% when compared to spray-dried solid dispersions, and is more evident with increasing polymer content as expected.

The experimental results obtained in this study motivate further work and provide directions for future experimental and theoretical work to consolidate the potential of dense gas antisolvent precipitation technology in pharmaceutical applications, and in the area of bioavailability enhancement of poorly water-soluble compounds in particular. Form a pharmaceutical point of view, it would be desirable to extend the present study, e.g., to higher polymer contents, to optimize the dissolution performance. Once product quality is optimized and mid- to long-term stability of PCA-processed solid dispersions has been duly checked and demonstrated, it will then be desirable to assess also the in vivo performance. From the technological point of view, it is decisive to further improve the fundamental understanding of the physical phenomena governing compressed fluid antisolvent precipitation to fully exploit its potential in future applications and eventually make the technology reach the market.

Acknowledgements

The authors gratefully acknowledge Kurt Schafflützel (Novartis Pharma AG) for technical support, continuous troubleshooting, and help with the PCA experiments, Philipp Heiny (Novartis Pharma AG) for running the spray drying experiments, Kurt Paulus and Dirk Märtin (Novartis Pharma AG) for performing the SEM analysis of the PCA precipitates, Martin Frei and Edgar John (Novartis Pharma AG) for valuable support in developing suitable methods for PSD measurements using laser light diffraction, and Christian Kirchhoffer (Novartis Pharma AG) for running the residual solvent content measurements of the PCA precipitates by GC and HPLC chromatography. Finally, we thank Andrea Kramer (Novartis Pharma AG), Ruth Alder and Bruno Gander (Institute of Pharmaceutical Sciences, ETH Zurich) for valuable discussions and scientific support.

References

Adrian, T., Maurer, G., 1997. Solubility of carbon dioxide in acetone and propionic acid at temperatures between 298 K and 333 K. J. Chem. Eng. Data 42, 668–672.

Bodmeier, R., Wang, H., Dixon, D.J., Mawson, S., Johnston, K.P., 1995. Polymeric microspheres prepared by spraying into compressed carbon dioxide. Pharm. Res. 12, 1211–1217.

Bleich, J., Müller, B.W., Wassmus, W., 1993. Aerosol solvent extraction system—a new microparticle production technique. Int. J. Pharm. 97, 111–117.

Bleich, J., Kleinebudde, P., Müller, B.W., 1994. Influence of gas density and pressure on microparticles produced with the ASES process. Int. J. Pharm. 106, 77–84.

Bleich, J., Müller, B.W., 1996. Production of drug loaded microparticles by the use of supercritical gases with the aerosol solvent extraction system (ASES) process. J. Microencapsul. 13, 131–139.

Bitz, C., Doelker, E., 1996. Influence of the preparation method on residual solvents in biodegradable microspheres. Int. J. Pharm. 131, 171–181.

Bungert, B., Sadowski, G., Arlt, W., 1998. Separations and materials processing in solutions with dense gases. Ind. Eng. Chem. Res. 37, 3208–3220.

Debenedetti, P.G., Tom, J.W., Yeo, S.D., Lim, G.B., 1993. Application of supercritical fluids for the production of sustained delivery devices. J. Control. Release 24, 27–44.

Dernell, W.S., Withrow, S.J., Kuntz, C.A., Dewell, R., Garry, F.B., Powers, B.E., Shively, J.E., Meyer, J.D., Manning, M.C., Falk, R.F., Randolph, T.W., 2001. In vivo evaluation of gentamycin impregnated polylactic acid beads implanted in sheep. J. Bioact. Compat. Polym. 16, 119–135.

Dukhin, S.S., Zhu, C., Dave, R., Pfeffer, R., Luo, J.J., Chavez, F., Shen, Y., 2003. Dynamic interfacial tension near critical point of a solvent-anisolvent mixture and laminar jet stabilization. Colloids Surf. A: Physicochem. Eng. Aspects 229, 181–199.

Elvassore, N., Baggio, M., Pallado, P., Bertucco, A., 2001. Production of different morphologies of biocompatible polymeric materials by supercritical CO_2 antisolvent techniques. Biotechnol. Bioeng. 73, 449–457.

Elvassore, N., Bertucco, A., Caliceti, P., 2001. Production of insulin-loaded poly(ethylene glycol)/poly(L-lactide)(PEG/PLA) nanoparticles by gas antisolvent techniques. J. Pharm. Sci. 90, 1628–1636.

Elvassore, N., Bertucco, A., Caliceti, P., 2001. Production of protein-loaded polymeric microcapsules by compressed CO_2 in a mixed solvent. Ind. Eng. Chem. Res. 40, 795–800.

Falk, R., Randolph, T.W., Meyer, J.D., Kelly, R.M., Manning, M.C., 1997. Controlled release of ionic compounds from poly(L-lactic acid) microspheres produced by precipitation with a compressed antisolvent. J. Control. Release 44, 77–85.

Fusaro, F., Hänchen, M., Mazzotti, M., Muhrer, G., Subramaniam, B., 2005. Dense gas antisolvent precipitation: a comparative investigation of the GAS and PCA techniques. Ind. Eng. Chem. Res. 44, 1502–1509.

Fusaro, F., Muhrer, G., Mazzotti, M., 2004. Gas antisolvent recrystallization of paracetamol from acetone using compressed carbon dioxide as antisolvent. Cryst. Growth Des. 4, 881–889.

Foster, N., Mammucari, R., Dehghani, F., Barrett, A., Bezanehtak, K., Coen, E., Combes, G., Meure, L., Ng, A., Regtop, H.L., Tandya, A., 2003. Processing pharmaceutical compounds using dense gas technology. Ind. Eng. Chem. Res. 42, 6476–6493.

Ghaderi, R., Artursson, P., Carlfors, J., 2000. A new method for preparing biodegradable microparticles and entrapment of hydrocortisone in DL-PLG microparticles using supercritical fluids. Eur. J. Pharm. Sci. 10, 1–9.

Ghaderi, R., Artursson, P., Carlfors, J., 1999. Preparation of biodegradable microparticles using solution-enhanced dispersion by supercritical fluids (SEDS). Pharm. Res. 16, 676–681.

Juppo, A.M., Boissier, C., Khoo, C., 2003. Evaluation of solid dispersions particles preapred by SEDS. Int. J. Pharm. 250, 385–401.

Jung, J., Perrut, M., 2001. Particle design using supercritical fluids: literature and patent survey. J. Supercrit. Fluids 20, 179–219.

Lin, C., Muhrer, G., Mazzotti, M., Subramaniam, B., 2003. Vapor–liquid mass transfer during gas antisolvent recrystallization: modeling and experiments. Ind. Eng. Chem. Res. 42, 2171–2182.

Lengsfeld, C.S., Delplanque, J.P., Barocas, V.H., Randolph, T.W., 2000. Mechanism governing microparticle morphology during precipitation by a compressed antisolvent: atomization vs. nucleation and growth. J. Phys. Chem. B 104, 2725–2735.

Müller, M., Meier, U., Kessler, A., Mazzotti, M., 2000. Experimental study of the effect of process parameters in the recrystallization of an organic compound using compressed carbon dioxide as antisolvent. Ind. Eng. Chem. Res. 39, 2260–2268.

Muhrer, G., Mazzotti, M., 2003. Precipitation of lysozyme nanoparticles from dimethyl sulfoxide using carbon dioxide as antisolvent. Biotechnol. Prog. 19, 549–556.

Muhrer, G., Mazzotti, M., Müller, M., 2003. Gas antisolvent recrystallization of an organic compound. Tailoring product PSD and scaling-up. J. Supercrit. Fluids 27, 195–203.

Muhrer, G., Lin, C., Mazzotti, M., 2002. Modeling the gas antisolvent recrystallization process. Ind. Eng. Chem. Res. 41, 3566–3579.

Meyer, J.D., Falk, R.D., Kelly, R.M., Shively, J.E., Withrow, S.J., Dernell, W.S., Kroll, D.J., Randolph, T.W., Manning, M.C., 1998. Preparation and in vitro characterization of gentamycin-impregnated biodegradable beads suitable for treatment of osteomyelitis. J. Pharm. Sci. 87, 1149–1154.

Moneghini, M., Kikic, I., Voinovich, D., Perissutti, B., Filipovic-Grcic, J., 2001. Processing of carbamazepine-PEG 4000 solid dispersions with supercritical carbon dioxide: preparation, characterisation, and in vitro dissolution. Int. J. Pharm. 222, 129–138.

Meure, L.A., Warwick, B., Dehghani, F., Regtop, H.L., Foster, N.R., 2004. Increasing copper indomethacine solubility be coprecipitation with poly(vinylpyrrolidone) using the aerosol solvent extraction system. Ind. Eng. Chem. Res. 43, 1103–1112.

Mawson, S., Kanakia, S.K., Johnston, K.P., 1997. Coaxial nozzle for control of particle morphology in precipitation with compressed antisolvent. J. Appl. Polym. Sci. 64, 2105–2118.

Perrut, M., Jung, J., Leboeuf, F., 2005. Enhancement of dissolution rate of poorly-soluble active ingredients by supercritical fluid processes. Part I. Micronization of neat particles. Int. J. Pharm. 288, 3–10.

Perrut, M., Jung, J., Leboeuf, F., 2005. Enhancement of dissolution rate of poorly-soluble active ingredients by supercritical fluid processes. Part II. Preparation of composite particles. Int. J. Pharm. 288, 11–16.

Ruchatz, F., Kleinebudde, P., Müller, B.W., 1997. Residual solvents in biodegradable microparticles. Influence of process parameters on the residual solvent in microparticles produced by the aerosol solvent extraction system (ASES) process. J. Pharm. Sci. 86, 101–105.

Randolph, T.W., Randolph, A.D., Mebes, M., Yeung, S., 1993. Sub-micrometer-sized biodegradable particles of poly(L-lactic acid) via the gas antisolvent spray precipitation process. Biotechnol. Prog. 9, 429–435.

Reverchon, E., Della Porta, G., De Rosa, I., Subra, P., Letourneur, D., 2000. Supercritical antisolvent micronization of some biopolymers. J. Supercrit. Fluids 18, 239–245.

Serajuddin, A.T.M., 1999. Solid dispersion of poorly water-soluble drugs: early promises, subsequent problems, and recent breakthroughs. J. Pharm. Sci. 88, 1058–1066.

Sekiguchi, K., Obi, N., 1961. Studies on absorption of eutectic mixture. I. A comparison of the behavior of eutectic mixture of sulfathiazole and that of ordinary sulfathiazole in man. Chem. Pharm. Bull. 9, 866–872.

Shariati, A., Peters, C.J., 2003. Recent developments in particle design using supercritical fluids. Curr. Opin. Solid State Mater. Sci. 7, 371–383.

Söhnel, O., Garside, J., 1992. Precipitation: Basic Principles and Industrial Applications, first ed. Butterworth-Heinemann, Oxford.

Shekunov, B.Y., Hanna, M., York, P., 2001. Crystallization process in turbulent supercritical flows. Chem. Eng. Sci. 198–199, 1345–1351.

Shekunov, B.Y., Baldyga, J., York, P., 2001. Particle formation by mixing with supercritical antisolvent at high Reynolds numbers. Chem. Eng. Sci. 56, 2421–2433.

Taki, S., Badens, E., Charbit, G., 2001. Controlled release system formed by supercritical anti-solvent coprecipitation of a herbicide and a biodegradable polymer. J. Supercrit. Fluids 21, 61–70.